

# Nanomechanical Properties of Cement Paste Containing Silica Fume

Salim Barbhuiya<sup>1</sup>, PengLoy Chow<sup>1</sup> and Arnesh Das<sup>2</sup>

<sup>1</sup> Curtin University Australia

<sup>2</sup> Delhi Technological University India

**Abstract:** *The recent emphasis on sustainability in the construction industry, and the growing requirements for ultra high strength and high performance concrete has dramatically increased the amount of research on effective substitutes for cement powder. In recent times major progress in the performance of concrete has been achieved with the use of silica fume (SF) as a cement substitute in concrete. However, the performance increase of concrete containing SF is limited by the lack of knowledge on the microstructural and nanomechanical properties of the cement paste. This research aims to provide a better understanding of the effects of SF on the nanomechanical properties of the main phases present within the cement paste. Three different mixes were prepared by replacing cement with silica fume at 0%, 5% and 10%. A constant water-binder ratio of 0.4 was used for all the mixes. Fraction volumes determined from nanoindentation testing show an increase in the porous phase of cement pastes containing SF due to agglomeration.*

**Keywords:** *silica fume, nanoindentation, Young's modulus, indentation hardness*

## 1. Introduction

Concrete is now the second most consumed substance on Earth, beaten only by water. It is used by the construction industry in large quantities throughout the world due to its high performance, relatively cheap price, and readily available raw materials. Over the past 100 years, there has been major progress in the performance and quality of concrete through scientific innovations [1]. However, little is still known about the microstructural and nanomechanical properties of concrete which is said to govern its overall properties such as strength and durability. The use of cement substitutes has gradually improved the mechanical properties of cement in recent, but this has been achieved more by trial and error than by an in-depth understanding of what is happening at the nano-scale

Silica fume (SF) is a by-product of the silicon or ferrosilicon alloy steel manufacturing process as a result of the high-purity quartz reduction with coal in electric furnaces [2]. SF is a fine powder with spherical particles of diameters ranging from 0.1-1.0 microns. SF also has a high surface area ranging from 15,000-25,000m<sup>2</sup>/kg [3]. These properties refine the void system of the cement paste and the interfacial zone [4]. These chemical properties make it a very reactive pozzolan. The pozzolanic reaction is a chemical reaction, which transforms the weaker Ca(OH)<sub>2</sub> crystals produced by the hydration of the Portland cement into additional C-S-H gel. At a microscopic level the formation of secondary C-S-H during a pozzolanic reaction bridges gaps between cement grains and aggregate particles, increases strength and reduces the permeability by increasing the density of the concrete matrix. High compressive strength is generally the first property associated with SF concrete. The addition of SF to a concrete mix increases the strength of that mix by between 30% and 100% depending on the type of mix, type of cement, amount of SF, use of superplasticisers, aggregate types and curing regimes.

This research aims to provide the industry with a better understanding of the effects of SF on the nanomechanical properties of the Calcium Silicate Hydrate (C-S-H) gel and other main phases within the cement paste. Current trends in concrete science and engineering aim to better define the properties of a concrete at different length scales. In doing so it would become possible to determine the macroscopic material properties

with a greater confidence by up scaling the properties determined at the micro or nano-scale. This can be achieved by a theoretical model or use of chemical equilibrium states to determine the properties, both of which rely on data on the nanomechanical properties of a cement paste. The research carried out here is critical to further define the effects of SF on a cement paste and ultimately help towards the development and optimisation of high strength concretes containing SF.

## 2. Experimental Programme

### 2.1. Materials

Cement powder used was a General Purpose Grey Portland Cement supplied by Cockburn Cement of Western Australia and certified to AS 3972 for general purpose and blended cements. Silica fume was Rheomac SF 100 and was supplied by BASF Chemicals in Perth. Typical chemical composition of cement and SF are given in Table 1.

TABLE I: Chemical Composition of Cement and Silica Fume

Oxides (%)	SiO <sub>2</sub>	Al <sub>2</sub> O <sub>3</sub>	Fe <sub>2</sub> O <sub>3</sub>	CaO	MgO	SO <sub>3</sub>	LOI	Chloride	Na <sub>2</sub> O Equivalent
OPC	21.1	4.7	2.8	63.8	2.0	2.5	2.1	0.01	0.50
Silica fume	97.8	-	-	-	-	0.3	1.4	0.02	0.001

### 2.2. Sample Preparation

The water-binder ratio (W/B) for all the mixes was kept constant at 0.4. Samples were prepared by cutting, setting, grinding and polishing the cement paste samples into cube of approximately 10mm size. Cutting of samples was carried out in two steps, the larger cuts were made by a tile cutter until the sample was small enough to be placed in the IsoMet 1000 Precision Saw for finer cuts. Samples were cast into moulds using a two-part resin consisting of Epoxy Resin and Epoxy Hardener. Grinding was carried on a Buehler AutoMet 250 in four steps of reducing diamond carbide paper roughness: 240, 360, 800 and 1200 grit, equivalent to 52.2, 35.0, 21.8 and 15.3µm respectively. Samples were ground with the 240 grit paper to expose the surface of the cement paste that may have been covered during the resin casting procedure (Fig. 1). At this point samples were then impregnated with EpoThin Epoxy Resin.

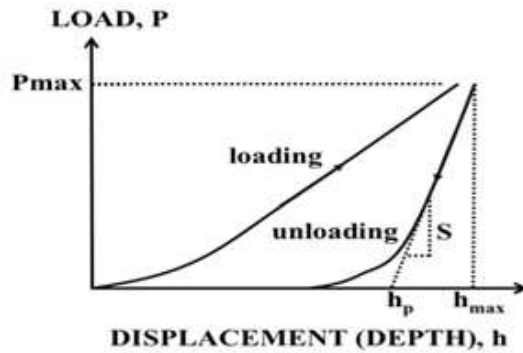


Fig. 1: Grinding and polishing of samples

After sample impregnation was complete the sample was ground down once again with the 240 grit paper. Once the surface was exposed, the 360 grit paper was used until the larger scratch marks of the previous paper are no longer visible. This process is repeated through the remaining grinding paper grits of 800 and 1200. Samples were polished on Buehler AutoMet 250 grinder-polisher using a polycrystalline diamond suspension of varying roughness; 9, 6, 3, 1, 0.25, 0.1µm. All samples were polished with an applied force of 20N for 5 minutes on each particle size with the exception of the 9µm that was applied for 10 minutes. All diamond suspension was set on a Buehler Texmat polishing cloth and supplemented with MediFluid fluid as the lubricant.

### 2.3. Test Methods

A typical outcome of the nanoindentation testing is an indentation load-depth hysteresis curve as shown in Fig. 1. As a load is applied to an indenter in contact with a specimen surface, an indent/impression is produced which consists of permanent/plastic deformation and temporary/elastic deformation. Recovery of the elastic deformation occurs when unloading is started. Determination of the elastic recovery by analysing the initial part of the unloading data according to a model for the elastic contact problem leads to a solution for calculation of the elastic modulus E and hardness H of the test area.



$$S = \frac{dP}{dh} = \frac{2}{\sqrt{\pi}} E_r \sqrt{A}$$

$$\frac{1}{E_r} = \frac{(1-\nu^2)}{E} + \frac{(1-\nu_i^2)}{E_i}$$

Fig. 1: indentation load-depth hysteresis curve

The nanoindentation apparatus used in this study was Nanoindenter XP (MTS Systems Corporation). In this study, all testing was programmed in such a way that the loading started when the indenter came into contact with the test surface and the load maintained for 30 seconds at the pre-specified maximum value before unloading. The unloading data for the lower indentation depth (i.e.  $h_p = 300\text{--}400$  nm) was used to determine the modulus and hardness values of the indentation point.

Information on the mechanical properties was obtained from a matrix of a minimum of 320 indents on the surface for cement paste samples. The selected indent spacing was  $20\ \mu\text{m}$ . The micro-mechanical properties of specific individual phases were extracted by statistically analysing all the test results, using a method similar to that presented by Constantinides et al., 2006 [5]. Basically, the experimental data (i.e. modulus and hardness values) were statistically analysed to produce a frequency histogram. Then, the best model fit to the experimental results with multimodal normal distribution curves (also known as Gaussian distribution, Eq. 1) was produced using nonlinear least squares method.

$$f(x; \mu, \sigma) = \frac{1}{\sigma\sqrt{2\pi}} \exp\left(-\frac{(x - \mu)^2}{2\sigma^2}\right) \quad (1)$$

From each model fit, the mean value  $\mu$  and standard deviation  $\sigma$  of the distribution were extracted. The area under the normal distribution curve could also provide an estimate of the volume fraction for the hydrate/mineral phase it associated with, within the area of the sample covered by indents. Grid indentation testing technique was used to ensure a representative set of data was collected of the cement paste samples. The selected method of grid indentation for this research was a  $4 \times 10$  indents per area. On each sample the grid indentation was repeated 8 times for a total of up to 320 indentation tests per sample. Each test area was selected by manual inspection using the indenters built in microscope. Analysis of the 320 data points per sample was done by the statistical deconvolution technique. The method was adopted from the indentation analysis by Constantinides et al., 2006 [5] and Sorelli et al., 2008 [6]. An algorithm was used to obtain the maximum likelihood estimates of the parameters in a Gaussian distribution model using the Solver program and spreadsheet. The number of phases for the analysis was set to four, one for each phase assumed to be within the cement paste, porous phase, LD C-S-H phase, HD C-S-H phase and the CH phase.

### 3. Results and Discussion

The faction volumes are calculated using the model distribution curves in combination with the theoretical line of best fit by calculating the area under each distribution. A summary of the results has been tabulated for each test result and can be seen in Table 2.

TABLE II: Modulus of Elasticity and Hardness Values for 90day Samples

Mix	Phase	Modulus		Hardness		Fraction Volume (%)
		Mean (GPa)	SD (GPa)	Mean (GPa)	SD (GPa)	
Control	Porous Phase	11.16	3.79	0.15	0.10	11%
	LD C-S-H	20.39	4.16	0.41	0.12	18%
	HD C-S-H	32.00	4.45	0.94	0.24	43%
	CH	47.34	5.50	1.50	0.23	29%
5% SF	Porous Phase	9.46	2.54	0.21	0.08	42%
	LD C-S-H	15.55	2.99	0.42	0.13	45%
	HD C-S-H	23.76	1.51	0.77	0.09	6%
	CH	31.98	4.66	1.09	0.23	6%
10% SF	Porous Phase	9.76	3.27	0.22	0.12	39%
	LD C-S-H	15.95	2.59	0.45	0.11	36%
	HD C-S-H	23.73	3.13	0.73	0.14	20%
	CH	33.82	2.09	1.10	0.08	5%

The visual representation of the statistical deconvolution results for modulus and hardness for the 90day control sample are presented in Figs. 2 and 3. The porous phase is a representation of the porosity of the sample. The reduction of the porous phase in cement pastes containing SF is typically attributed to the reduced amount of voids within the cement matrix as a result of the very fine SF particles filling the empty voids between the hydrated cement particles. Furthermore, the inclusion of SF in a cement paste is suggested to cause a pozzolanic reaction, turning calcium hydroxide into additional C-S-H. C-S-H has a much greater volume than the calcium hydroxide phase that it replaces, as the volume of the cement paste itself does not change, the increased volume of C-S-H gel should reduce the porosity of the cement matrix. However, in review of these results it can be seen that there is a large increase, approximately 4 times, in the fraction volume of the porous phase of the samples containing SF. This contradicts the expected findings as it implies that the porosity of cement paste has increased with the inclusion of SF.

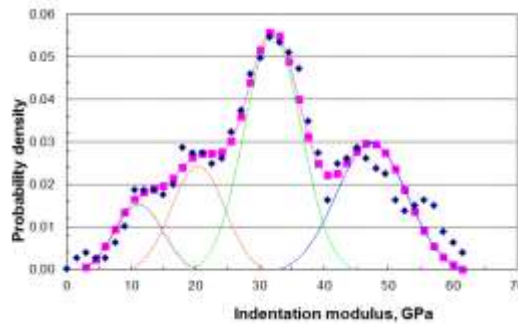


Fig. 2: Probability Distribution Curve for Modulus for 90day Control Sample

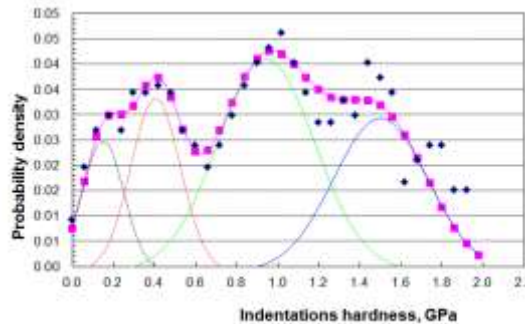


Fig. 3: Probability Distribution Curve for Hardness for 90day Control Sample

This variation could be a result of experimental error, however it is more likely a result of the SF not being completely dispersed throughout the cement paste. Previous research has reported issues with the dispersion and agglomeration of the SF particles within the cement paste [7]. Agglomeration of the SF particles would cause them to stick together and not effectively react with the cement particles, instead forming small areas of high porosity and ultimately a low modulus of elasticity, which may be the cause of the results shown within this report.

Both the LD C-S-H and HD C-S-H phases across all samples show erratic variations. As suggested previously, the expected result here is that the addition of SF increases the volume of C-S-H present in the sample and that an increase of the HD C-S-H should be observed. Immediately it can be seen that this is not the case with the results showing a dramatic decrease in the fraction volume of the HD C-S-H in both samples containing SF. Furthermore, the total fraction volume of the combined C-S-H is less in the SF samples than it is in the control. These results not only imply that the inclusion of SF into a cement paste reduces the amount of HD C-S-H within the sample, it also suggests that SF reduces the total amount of C-S-H within the sample.

The variation in the fraction volume like all other aspects of nanoindentation testing could be a result of sample preparation and testing errors. However, it is likely that the erratic modulus values are a result of one of the following two factors. The first being that the suggested agglomeration within the SF samples has reduced the effectiveness of the pozzolanic reaction, in turn reducing the amount of HD C-S-H produced. Or an unrepresentative section of the cement paste sample has been selected during testing. Site selection for the nanoindentation was carried out manually by inspection using the inbuilt microscope. Upon review of the samples under the microscope it became evident that the samples contained areas that were either not flat, or contained small voids on the surface. As a result of this, test sites were selected based on areas that appeared to be flat, well polished, and free of surface raises or voids. In doing this it is possible that the selected sites for testing were more representative of the lower hardness phases within the sample. The porous and LD C-S-H phases with a lower hardness value would be more susceptible to the grinding and polishing process resulting in a much smoother and flatter surface like the areas selected for testing.

Literature on hardness of cement paste phases stated the approximate values of porous, LD C-S-H, HD C-S-H, and CH as 0.17, 0.45, 0.83, and 1.31GPa respectively [8]. The results reported here correlate closely with the literature results, with the exception of the HD C-S-H and CH phases of the control. The increased hardness of the cement paste at the macro level could be related to the increased volume of the harder phases present in the sample, rather than the increase in the hardness of the individual phases, however variation in the fraction volumes of the hardness phases means no conclusion can be drawn.

## 4. Conclusions

Fraction volumes of the porous phase in the samples containing silica fume were approximately 4 times that of the control sample. This can be attributed to the fact that silica fume is not completely dispersed throughout the cement paste. Erratic C-S-H gel modulus volumes were attributed to two factors; the increase of the porous phase as a result of agglomeration and an unrepresentative section of the cement paste sample being selected for as a result on manual site selection.

## 5. References

- [1] Mondal, P., Shah, S.P., Marks, L.D., "Nanoscale Characterisation of Cementitious Materials", *ACI Materials Journal*, 2008, Vol. 105 (2), pp. 174-179.
- [2] Siddique, R., "Utilization of Silica Fume in Concrete: Review of Hardened Properties", *Resources, Conservation and Recycling*, 2011, Vol. 55 (11), pp. 923-932.  
<http://dx.doi.org/10.1016/j.resconrec.2011.06.012>
- [3] Dunster, A., *Silica Fume in Concrete*. Watford: BRE Publications, 2009, 25pp.
- [4] Toutanji, H.A. and Bayasi, Z., "Effect of Curing Procedures on Properties of Silica Fume Concrete", *Cement and Concrete Research*, 1999, Vol. 29 (4), pp. 497-501.  
[http://dx.doi.org/10.1016/S0008-8846\(98\)00197-5](http://dx.doi.org/10.1016/S0008-8846(98)00197-5)
- [5] Constantinides, G., Ravi Chandran, K.S., Ulm, F.J. and Van Vliet, K.J., "Grid Indentation Analysis of Composite Microstructure and Mechanics: Principles and Validation", *Materials Science and Engineering: A*, 2006, Vol. 430 (1-2), pp. 189-202.  
<http://dx.doi.org/10.1016/j.msea.2006.05.125>
- [6] Sorelli, L., Constantinides, G., Ulm, F.J., and Toutlemonde, F., "The Nano-Mechanical Signature of Ultra High Performance Concrete by Statistical Nanoindentation Techniques", *Cement and Concrete Research*, 2008, Vol. 38 (12), pp. 1447-1456.  
<http://dx.doi.org/10.1016/j.cemconres.2008.09.002>

- [7] Yajun, J. and Cahyadi, J.H., “Effects of Densified Silica Fume on Microstructure and Compressive Strength of Blended Cement Pastes”, *Cement and Concrete Research*, 2003, Vol. 33 (10), pp. 1543-1548.  
[http://dx.doi.org/10.1016/S0008-8846\(03\)00100-5](http://dx.doi.org/10.1016/S0008-8846(03)00100-5)
- [8] Constantinides, G. and Ulm, F.J., “The Nanogranular Nature of C–S–H”, *Journal of the Mechanics and Physics of Solids*, 2007, Vol. 55 (1), pp. 64-90.  
<http://dx.doi.org/10.1016/j.jmps.2006.06.003>